

Energy, Exergy, and Environmental Emission Analysis of a Crude Oil-Fired AL-Musayib Thermal Station in Iraq

Hasnaa A. Majed, Ammar A. Farhan*

Department of Energy Engineering, College of Engineering, University of Baghdad, Baghdad, Iraq

ARTICLE INFO

Article history:

Received August 18, 2024
Revised October 18, 2024,
Accepted November 29, 2024,
Available online December 1, 2024

Keywords:

Crude oil-fired
Energy
Environmental emission
Steam power plant

ABSTRACT

The analysis of steam power plants (SPPs) based on the first and second laws of thermodynamics is crucial for evaluating both the quantity and quality of energy sources. In this study, the energetic and exergetic efficiencies of a 200 MW crude oil-fired SPP were analyzed using ASPEN HYSYS software. The objective was to assess the plant's performance and examine the impact of varying ambient temperatures on each component of the SPP. Additionally, crude oil-fueled SPPs are significant sources of CO₂ and SO₂ emissions, contributing to global warming and environmental degradation. Therefore, the quantities of these emissions were calculated, and their relationship with ambient temperature was evaluated. Energy losses and exergy destruction were also determined for each component to identify key areas for improvement. Results showed that both energetic and exergetic efficiencies decreased with rising ambient temperatures. At an ambient temperature of 20°C, the energetic efficiency was 33.9%, and the exergetic efficiency was 32.89%. Findings revealed that the condenser accounted for approximately 56.16% of the total energy loss, while the boiler had an exergy destruction rate of 84.14%. In addition, as the ambient temperature increased from 20°C to 45°C, CO₂ emissions rose from 51.8 kg/h to 56.9 kg/h, while SO₂ emissions increased from 1.02 kg/h to 1.03 kg/h.

1. Introduction

Energy is a vital component of every country's modern economy, supporting sectors such as transportation, industry, agriculture, and domestic needs. Currently, 80% of the world's electricity is generated by fossil fuel-powered power plants, while the remainder comes from alternative energy sources like hydroelectric, solar, nuclear, and wind power [1–3]. The growing global demand for energy has led to an overreliance on steam power plants that burn fossil fuels, accounting for approximately 65% of the world's electricity production [4].

The energy efficiency of steam power plants has been extensively studied using the 1st law of

thermodynamics. However, this law only evaluates the quantity of energy, without differentiating between energy quantity and quality, and therefore cannot provide a comprehensive view of actual useful energy losses [5]. In recent decades, energy analysis based on the 2nd law of thermodynamics has gained prominence as a more effective approach for planning, estimating, optimizing, and enhancing steam power plants [6].

Exergy analysis, which is based on the 2nd law, allows for a detailed assessment of energy quality and utility by identifying sources of high irreversibility within each component of the power cycle. This provides crucial insights into the system's

* Corresponding author.

E-mail address: ammarali@uobaghdad.edu.iq

DOI: [10.24237/djes.2024.17403](https://doi.org/10.24237/djes.2024.17403)

This work is licensed under a [Creative Commons Attribution 4.0 International License](https://creativecommons.org/licenses/by/4.0/).



performance [7]. Furthermore, it simplifies the process of quantifying the loss of usable work overtime and under varying operating conditions [8]. By evaluating both energy efficiency and losses, it can pinpoint areas for improvement and optimization in energy conversion processes [9].

The energy and exergy performance of the 200 MW Shahid Montazeri Power Plant was analyzed through numerical simulations. The study investigated how varying the number of feed water heaters impacts the plant's efficiency. Findings revealed energy and exergy efficiencies of 37.52% and 41.7%, respectively, with the combustion chamber contributing approximately 48% to the total exergy destruction [10]. Khalil et al. [11] conducted a parametric analysis to evaluate plant efficiency, focusing on the impact of varying coal consumption and the number of feedwater heaters, which significantly contribute to exergy destruction. The study found that exergy destruction rose by 16% with a 40 kg/s increase in fuel consumption, while elevated coal usage also diminished the effectiveness of the feedwater heaters. A numerical code was developed using Engineering Equation Solver to analyze the power plant's performance under different operational conditions. The findings indicate that doubling the superheater pressure increases the net power output by more than 8%, while raising the superheated steam temperature from 539.8°C to 580°C leads to a power increase of over 6%. Conversely, increasing the reheater pressure from 30 to 34 bar results in a 1.57% reduction in net power output [12]. Ibrahim et al. [13] provided an in-depth review of thermodynamic analyses for combined cycle power plants, noting significant energy losses in the condenser and substantial exergy destruction in the combustion chamber. They emphasized exergy analysis as a crucial method for improving plant efficiency, minimizing fuel consumption, and lowering emissions.

Kumer et al. [14] emphasized the growing importance of exergy analysis for understanding process control and addressing modern energy security and sustainability challenges. Their study of a 210 MW integrated coal-fired thermal power plant found that about 64.24% of total

energy loss occurred in the condenser, while the boiler had an exergy destruction rate of 88.91%. Additionally, as the ambient temperature increased from 25°C to 45°C, coal consumption and ash generation per unit of fuel rose, leading to higher reductions in CO₂ and SO₂ emissions. Eke et al. [15] analyzed the performance of a 220 MW thermal power plant through energy and exergy analysis, utilizing the plant's design and operational data. Their findings revealed that the boiler was responsible for 87% of the total exergy destruction, while the three turbines contributed 9%, and the condenser accounted for 2% of the overall exergy destruction within the cycle. Kaushik et al. [16] provided a concise review of multiple studies comparing energy and exergy analyses of thermal power plants fueled by coal and gas. Their findings indicated that the primary exergy loss in coal-based power plants occurs in the boiler. Ameri et al. [17] conducted a comprehensive analysis that integrated both energy and exergy assessments for a steam power plant, highlighting the efficiencies and losses within the system. Meanwhile, Ghaebi et al. [18] carried out an in-depth energy, exergy, and thermo-economic analysis of a combined cooling, heating, and power system. Their work not only evaluated the performance metrics of the system but also examined the economic implications of energy utilization, offering insights into optimizing the overall efficiency and sustainability of combined energy systems. Al-Jundi [19] conducted a study on the impact of ambient temperature on energy efficiency in the Hussein steam power plant in Jordan. They found that increasing the temperature reduced thermal stress destruction, resulting in nearly double the efficiency of the condenser at 318.15 K. Ahmadi and Toghraie [20] examined the steam cycle of the Shahid Montazeri Power Plant in Isfahan, which features an individual unit capacity of 200 MW. Their findings reveal that 69.8% of the total energy loss occurs in the condenser, while the boiler is recognized as the primary source of exergy loss, contributing to 85.66% of the total exergy entering the cycle.

The aim of this work is to evaluate the energetic and exergetic efficiencies of a 200 MW crude oil-fired steam power plant (SPP)

using ASPEN HYSYS software, while examining the impact of varying ambient temperatures on different components of the plant. Additionally, the study seeks to quantify CO₂ and SO₂ emissions from the SPP and assess their relationship with ambient temperature. By determining energy losses and exergy destruction across the system, the research aims to identify key areas for improving plant performance. This work is important for addressing the environmental impact of crude oil-based power generation, particularly by understanding the link between emissions and temperature changes, and for optimizing energy efficiency to enhance overall system performance. The findings provide valuable insights for improving sustainability and reducing greenhouse gas emissions in fossil fuel-based power plants, offering practical data to guide engineers and plant operators in minimizing energy losses and operational costs.

1.1 Plant description cycle

AL-Musayib Steam Power is a 1200 MW power plant with four independent units. It is located 30 meters above sea level in the city of Babylon, 75 km south of Baghdad in Iraq. It began producing power in the mid-1970s. For the purposes of this analysis, only one unit from the integrated plant, which generates 2.0 MW of power, is considered. The power station's flow diagram is depicted in Figure 1, and the operational parameters of plant unit No. 1 are listed in Table 1. An overview of this cycle's heating process. Each unit in this power plant has a water-steam circuit as follows: At state point 12, 170°C and 166 bar of pressure are reached when feedwater enters the boiler. At state point 13, when it is 535°C and under 156 bar of pressure, it warms up to a superheated vapor and exits the boiler. The pressure then decreases from 156 bar to 30 bar when the superheated steam is added to the HPT. After being warmed in the boiler, the leftover steam is subsequently sent into the intermediate pressure turbine, from which some is drawn to the HPT at state point 18. Furthermore, some heat is removed at state points 35, 31, and 24. At state point 23, the Low-Pressure Turbine receives the

residual steam at a pressure of 3.8 bar and a temperature of 285°C. 85°C and 0.39 bar of pressure are present at state point 26, an extraction is carried out for Low-Pressure Heater-1 in the Low-Pressure Turbine. Following this, the steam is gathered in the condenser well and undergoes a single cooling cycle to become liquid. Water collected from the condenser well is sent into the CWP via this cycle. After going through Low-Pressure Heater-1, feedwater then passes via Low-Pressure Heaters 2, 3, and 4 to reach the deaerator. To remove O₂ and other dissolved gases, the feedwater in the deaerator is combined with steam that has been extracted from the HPT and Intermediate Pressure Turbine. The boiler is subsequently refilled with the deaerated feedwater.

2. Energy – exergy analysis

Two widely used techniques for assessing Steam power plant performance are energy-exergy assessments. Aspen HYSYS. software is used to solve all model equations based on unit-1 measurements, which are compiled in Table 1 to show the operating circumstances under which the 200 MW of electricity it generates is produced. This comprises the energy that comes from the crude oil as well as any losses brought on by systemic inefficiencies. The energy and exergy analysis's findings give a general overview of the power plant's energy efficiency and point out areas for improvement. To determine areas for improvement and to quantify the performance of each system component in a Steam power station, energy-exergy analysis can be performed. The steps and computations needed to do a 1st and 2nd law analysis of a Steam power plant is outlined in these equations [21]. The main focus is on the energy analysis section, this entails figuring out an open system steady flow process' energy equation [14–22].

$$\sum \dot{Q}_K + \dot{m} \left(h_i + \frac{C_i^2}{2} + gZ_i \right) = \dot{m} \left(h_o + \frac{C_o^2}{2} + gZ_o \right) + \dot{W} \quad (1)$$

$$\begin{aligned} \sum \left(1 - \frac{T_o}{T}\right) Q_K &= \sum (\dot{m}_i \psi_i) \\ &= \sum \psi_w \\ &+ \sum (\dot{m}_o \psi_o) \\ &+ I_{destroyed} \end{aligned} \quad (2)$$

Equations (1) and (2) may be used to describe the particular flow energy as [20,23], when they are equal.

$$\psi = (h - h_o) - T_o(s - s_o) \quad (3)$$

In contrast, the flow's total exergy equals [24].

$$Ex = \dot{m}\psi = \dot{m}(h - h_o) - T_o(s - s_o) \quad (4)$$

2.1. Energy-exergy for boiler

The main part of the power plant is the boiler, which generates steam by burning fuel. Calculating the energy intake from the crude oil and the energy output as steam is part of the boiler's energy analysis. The chemical energy of the fuel is liberated while burning and then transferred by the transmission of heat to the water. Nevertheless, the boiler's energy efficiency is reduced by partial fuel combustion brought on by a large temperature difference that occurs during the process of heat transfer [25]. This will allow for the computation of the exergy of all sites, including input and exit flows. To do this, we use equation (3) with specific values of enthalpy, entropy, and the ambient temperature. According to [17].

Each steam flow's unique exergy is computed. The boiler's energy efficiency and balance:

$$\begin{aligned} \dot{m}_f h_f + \dot{m}_a h_a &= \dot{m}_g h_g \\ &+ \dot{m}_{12}(h_{13} - h_{12}) \\ &+ \dot{m}_{17}(h_{18} - h_{17}) \\ &+ Q_{18} \end{aligned} \quad (5)$$

$$\eta_{1B} = \frac{\dot{m}_{12}(h_{13} - h_{12}) + \dot{m}_{17}(h_{18} - h_{17})}{\dot{m}_f h_f} \quad (6)$$

Exergy balance and efficiency of the boiler:

$$\begin{aligned} 0 &= \sum_{k=1}^r [(\dot{m}\psi)_{f+a} - (\dot{m}\psi)_p]_k \\ &= Exergyloss \end{aligned} \quad (7)$$

$$0 = [(\dot{m}\psi)_{f+a} - (\dot{m}\psi)_p]_k - Exergyloss \quad (8)$$

$$\begin{aligned} \eta_{II B} &= \frac{Exergy\ output}{Exergy\ input} \\ &= 1 - \frac{Exergy\ loss}{Exergy\ input} \end{aligned} \quad (9)$$

$$\begin{aligned} T_o \dot{S}_{gen} &= (\dot{m}_f \psi_f) + (\dot{m}_a \psi_{fa}) \\ &+ (\dot{m}_{12} \psi_{12}) \\ &+ (\dot{m}_{17} \psi_{17}) - (\dot{m}_g \psi_g) \\ &- (\dot{m}_{13} \psi_{13}) - (\dot{m}_6 \psi_6) \end{aligned} \quad (10)$$

$$\eta_{II B} = \frac{(\dot{m}_g \psi_g) + (\dot{m}_{13} \psi_{13}) + (\dot{m}_{18} \psi_{18})}{(\dot{m}_f \psi_f) + (\dot{m}_a \psi_{fa}) + (\dot{m}_{12} \psi_{12}) + (\dot{m}_{17} \psi_{17})} \quad (11)$$

2.2. Energy-exergy analysis for turbines

The steam's energy is transformed into mechanical energy by the turbines, which is subsequently utilized to produce electricity. Calculating the quantity of energy intake as steam and the quantity of energy output as mechanical energy is the first step in an energy analysis of the turbines. To evaluate the energy's quality and capacity for productive lab or, an exergy study is also carried out [24]. Three different types of turbines are employed at the AL-Musayib Steam Power Station: an HPT, an IPT, and a LPT. The energy-exergy efficiency is ascertained by first analysing each step separately in the energy-exergy analysis process. The following are the HPT energy and energy formula [26].

2.2.1. HPT energy-exergy analysis

Energy balance equation for HPT :

$$W_{HPT} = \dot{m}_{13}(h_{13} - h_{15}) + (\dot{m}_{13} - \dot{m}_{15})(h_{15} - h_{14}) - \text{Energyloss} \quad (12)$$

$$\eta_{I \text{ HPT}} = \frac{W_{HPT}}{\dot{m}_{13}(h_{13} - h_{15}) - (\dot{m}_{15} - \dot{m}_{14})(h_{15} - h_{14})} \quad (13)$$

Exergy balance equation for HPT :

$$W_{HPT} = \dot{m}_{13}(\psi_{13} - \psi_{15}) + (\dot{m}_{13} - \dot{m}_{15})(\psi_{15} - \psi_{14}) - I_{destroyed} \quad (14)$$

$$I_{destroyed} = T_0[(\dot{m}_{13}(s_{15} - s_{13}) + (\dot{m}_{13} - \dot{m}_{15})(s_{14} - s_{15}))] \quad (15)$$

$$\eta_{II \text{ HPT}} = \frac{W_{HPT}}{\dot{m}_{13}(\psi_{13} - \psi_{15}) + (\dot{m}_{13} - \dot{m}_{15})(\psi_{15} - \psi_{14})} \quad (16)$$

$$\eta_{II \text{ HPT}} = \frac{W_{HPT}}{\dot{m}_{13}(\psi_{13} - \psi_{15}) + (\dot{m}_{13} - \dot{m}_{15})(\psi_{15} - \psi_{14})} \quad (17)$$

2.3. Condenser energy-exergy analysis

A condenser converts steam energy into water by absorbing it from turbines. Its energy performance is determined by calculating steam's energy intake and cooling water's output [27]. High pressure and temperature steam enters the condenser, releasing latent heat and reheating it before returning to the environment. Irreversibility's cause part of the steam's energy to be lost throughout this process, though. The AL-Musayib Steam Power Station uses condensers of the direct spray type.

Energy balance for Condenser:

$$0 = \dot{m}_{27}(h_{27} - h_1) - Q_K - \text{Exergy loss} \quad (18)$$

$$\eta_{I \text{ c}} = 1 - \frac{\text{Exergy loss}}{\dot{m}_{27}(h_{27} - h_1)} \quad (19)$$

2.4. CFWH energy-exergy analysis

Heaters preheat FWB before reaching the boiler, assessing their energy efficiency by calculating the energy produced by steam and the energy resulting in warmed water [28]. Steam's higher temperature and pressure contribute to higher-quality energy, which enters the CFWH and is transferred to the water, warming it before reaching the boiler. Irreversibility's cause part of the steam's energy to be lost during the process, though [29]. Calculating the LPH1 energy balance involves:

$$0 = \dot{m}_{26}(h_{26} - h_{33}) - \dot{m}_{17}(h_3 - h_2) - \text{Exergy loss} \quad (20)$$

$$\eta_{I \text{ LPT1}} = \frac{\dot{m}_2(h_3 - h_2)}{\dot{m}_{26}(h_{19} - h_{33})} \quad (21)$$

Calculating the LPH1 exergy balance involves:

$$0 = \dot{m}_{26}(\psi_{26} - \psi_{33}) - \dot{m}_2(\psi_3 - \psi_2) - I_{destroyed} \quad (22)$$

$$I_{destroyed} = [\dot{m}_{26}(h_{26} - h_{33}) - \dot{m}_2(h_3 - h_2) - T_0(\dot{m}_{26}(s_{26} - s_{33}) - \{\dot{m}(s_3 - s_2)\})] \quad (23)$$

$$\eta_{II \text{ HPT1}} = 1 - \frac{I_{destroyed}}{\dot{m}_{26}(\psi_{26} - \psi_{33})} = \frac{\dot{m}_{17}(\psi_3 - \psi_{17})}{\dot{m}_{26}(\psi_{26} - \psi_{33})} \quad (24)$$

2.5. Analysis of energy-exergy in a deaerator

The deaerator functions as an open feed water heater in a power plant cycle, with equilibrium energy determined by the following equations[30].

$$0 = \dot{m}_7 h_7 + \dot{m}_{21} h_{21} + \dot{m}_{29} h_{29} + \dot{m}_{37} h_{37} + \text{Energyloss} \quad (25)$$

$$\eta_{I \text{ Deaerator}} = \frac{\dot{m}_8 h_{38}}{\dot{m}_7 h_7 + \dot{m}_{21} h_{21} + \dot{m}_{29} h_{29}} \quad (26)$$

Exergy balance for deaerator:

$$0 = \dot{m}_7\psi_7 + \dot{m}_{21}\psi_{21} + \dot{m}_{29}\psi_{29} - \dot{m}_8\psi_8 - I_{destroyed} \quad (27)$$

$$I_{destroyed} = T_0\{\dot{m}_7s_7 + \dot{m}_{21}s_{21} + \dot{m}_{29}s_{29} + \dot{m}_8s_8\} \quad (29)$$

$$I_{destroyed} = \dot{m}_7\psi_7 + \dot{m}_{21}\psi_{21} + \dot{m}_{29}\psi_{29} - \dot{m}_8\psi_8 \quad (28)$$

$$\eta_{II}^{Deaerator} = \frac{I_{destroyed}}{\dot{m}_7s_7 + \dot{m}_{21}s_{21} + \dot{m}_{29}s_{29} - \dot{m}_8s_8} = \frac{\dot{m}_7\psi_7 + \dot{m}_{21}\psi_{21} + \dot{m}_{29}\psi_{29} - \dot{m}_8\psi_8}{\dot{m}_7s_7 + \dot{m}_{21}s_{21} + \dot{m}_{29}s_{29} - \dot{m}_8s_8} \quad (30)$$

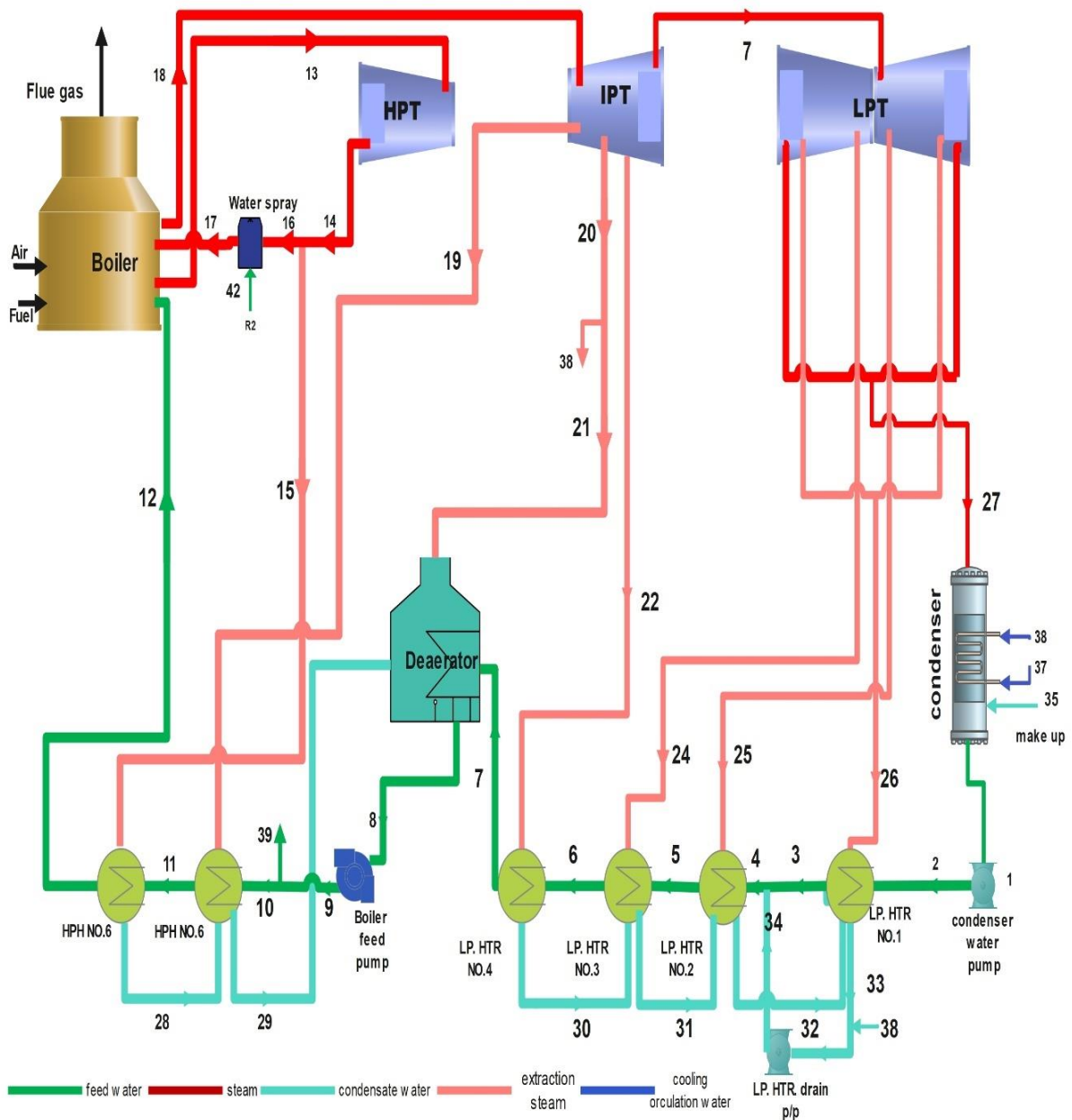


Figure 1. AL-Musayib Steam Power Station's plant schematic

Table 1: Thermodynamic properties of all the steam power plant data at AL-Musayib

Point	T (°C)	P (bar)	\dot{m} (kg/s)	h (kJ/kg)	S (kJ/kg.k)
1	43	0.1	149.9	191.8	0.6492
2	49	24	149.9	207.2	0.6898
3	64	24	149.9	269.9	0.8799
4	65	24	181.9	274.1	0.8923
5	89	24	181.9	374.6	1.18
6	110	24	181.9	463.1	1.417
7	137	24	181.9	577.7	1.706
8	167	5	190.6	640.1	1.86
9	170	166	190.6	727.9	2.022
10	170	166	179.8	727.9	2.022
11	170	166	179.8	727.9	2.022
12	170	166	179.8	727.9	2.022
13	535	156	178.7	3403	6.448
14	344	30.6	178.7	3101	6.711
15*	0	0	0	0	0
16	344	30	178.7	3102	6.722
17	324.7	30	182.2	3056	6.646
18	535	28.5	182.2	3537	7.36
19*	0	0	0	0	0
20	345	6.34	15.35	3155	7.505
21	345	6.34	8.611	3155	7.505
22	285	3.8	8.226	3037	7.538
23	285	3.8	158.7	3037	7.538
24	213	1.95	6.12	2897	7.575
25	130	0.81	6.769	2738	7.619
26	85	0.39	3.964	2654	7.732
27	41.6	0.1	141.8	2464	7.774
28*	0	0	0	0	0
29*	0	0	0	0	0
30	119.5	3.8	8.226	501.8	1.522
31	96	1.95	14.35	402.4	1.262
32	68	0.81	21.11	284.7	0.9306
33	68	0.81	25.08	284.7	0.9306
34	68	23	31.81	286.6	0.9293
35	30	0.8	6680	125.8	0.4367
36	35	0.8	6680	146.7	0.5051
37	20	6	8.056	84.48	0.2964
38	110	6.34	6.736	679.8	1.952
39	170	166	10.78	727.9	2.022
40	170	166	7.222	727.9	2.022
41	170	166	3.556	727.9	2.022
42	210	166	8.333	903.1	2.4

* Refers that the nodes shown without values because the high-pressure heaters (6 and 7) were out of service.

3. Environmental Mapping

All types of power plants, including Steam, hydroelectric, nuclear, solar, and others, have environmental effects. These effects, such as pollution and disturbances to ecosystems, are harmful and inevitable. Power is depended upon

for existence, but the increased energy is accompanied by environmental degradation or destruction. Therefore, reducing these detrimental consequences on the environment is imperative [31].

3.1. Analysis of environmental emissions from the burning of crude oil

Emissions from power plant have a detrimental effect on the environment and are extremely hazardous. Burning crude oil with a high oxide content in the flue gas produces greenhouse gases (GHGs) such CO₂, CO, Sox, and NO_x [32,33]. The amount of CO₂ emitted can be calculated using the carbon content of the crude oil. For each kilogram of fuel burned, a specific amount of CO₂ is produced based on the stoichiometric combustion equation:

$$\text{(Carbon Dioxide) CO}_2 \text{ emissions} = \text{fuel}_{a,b} \times \text{Carbon Content Fraction} \times \text{CO}_2 \text{ Emission factors} \quad (31)$$

Where:

Fuel = Fuel consumed in volume (e.g. gallons, liters, cubic meters, etc.) by fuel type for each energy, a = Fuel type (e.g. natural gas, coal, fuel oil, etc.), b = Energy type (electricity, heating, or cooling).

Carbon Content Fraction: Fraction of carbon in the fuel from Table 2.

CO₂ Emission Factor: Theoretical amount of CO₂ produced per kilogram of carbon burned (3.67 kg CO₂/kg C).

$$\text{SO}_2 \text{ emissions} = \text{fuel}_{a,b} \times \text{Sulfur Content Fraction} \times \text{SO}_2 \text{ Emission Factor} \quad (32)$$

Where:

Sulfur Content Fraction: Fraction of sulfur in the crude oil.

SO₂ Emission Factor: The amount of SO₂ produced per kilogram of sulfur burned (2 kg SO₂/kg S).

Table2: Crude oil analysis.

Component	Carbon	Hydrogen	Sulfur	Oxygen
Mass (%)	83.2	12.5	2	0.0

4. Results and Discussion

4.1. An energy-exergy study of the main steam power plant components

An energy-exergy study was conducted on the steam power plant's constituent parts at AL-Musayib in addition to environmental emission analyses. With 25 °C as the standard temperature and 101.3 kPa of pressure, a reference condition was set. The Aspen HYSYS programs was used to determine the explicit exergy and flow exergy values for each node location. Figures 2 and 3 illustrate the percentage distribution of energy losses at the actual operating load. The condenser accounts for the largest portion of energy losses, amounting to 181.76 MW, which represents 56.18% of the total energy losses in the cycle. This significant energy loss is primarily due to the substantial amount of heat energy expelled by the condenser into the atmosphere and the poor quality of steam at this stage.

The boiler is another major contributor to energy losses, accounting for 51.08 MW, or 15.79% of the total losses. This energy loss is largely attributed to combustion inefficiencies and heat transfer limitations inherent in crude oil-fired thermal power plants. The high-pressure turbine (HPT), intermediate-pressure turbine (IPT), and low-pressure turbine (LPT) also exhibit notable energy losses, although to a lesser extent than the condenser and boiler. Their respective losses are 27.50 MW (8.50%), 17.13 MW (5.29%), and 20.47 MW (6.33%) of the total energy losses in the cycle. Additionally, energy losses are observed in the boiler feed pump (BFP), cooling water pump (CWP), and deaerator. The BFP contributes 13.38 MW (4.14%) to the overall losses, the CWP accounts for 1.94 MW (0.60%), and the deaerator adds 10.29 MW (3.18%).

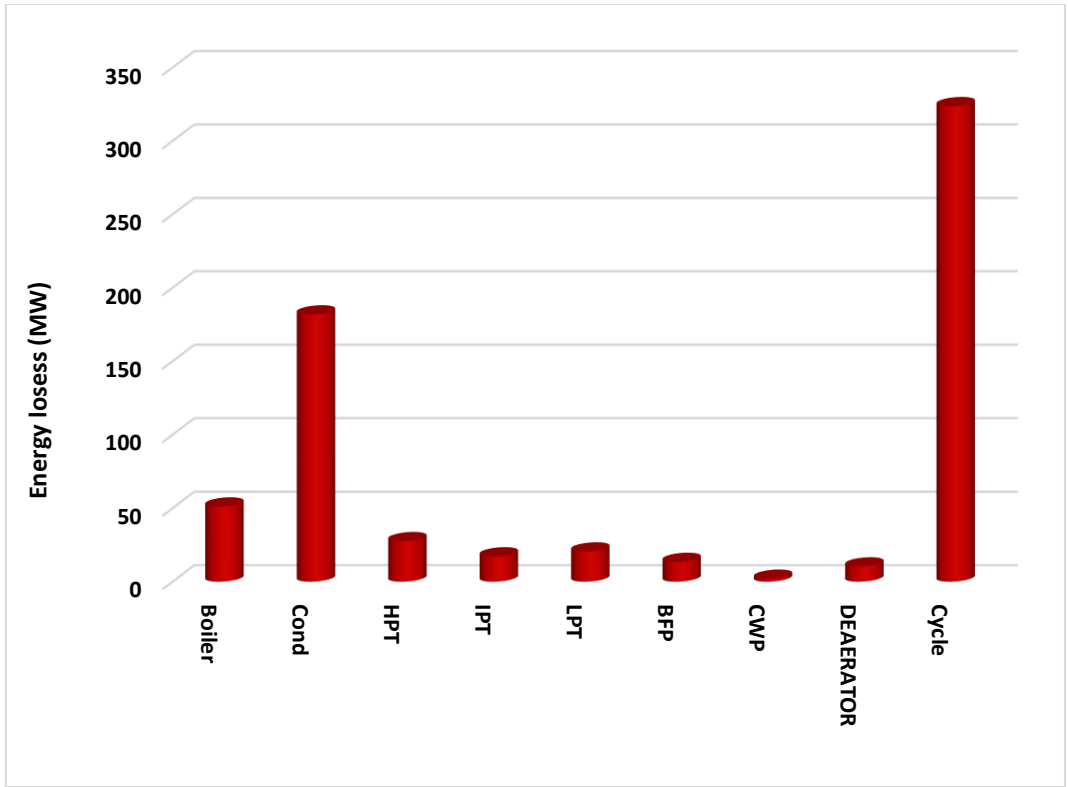


Figure 2. Energy losses distribution for rated load.

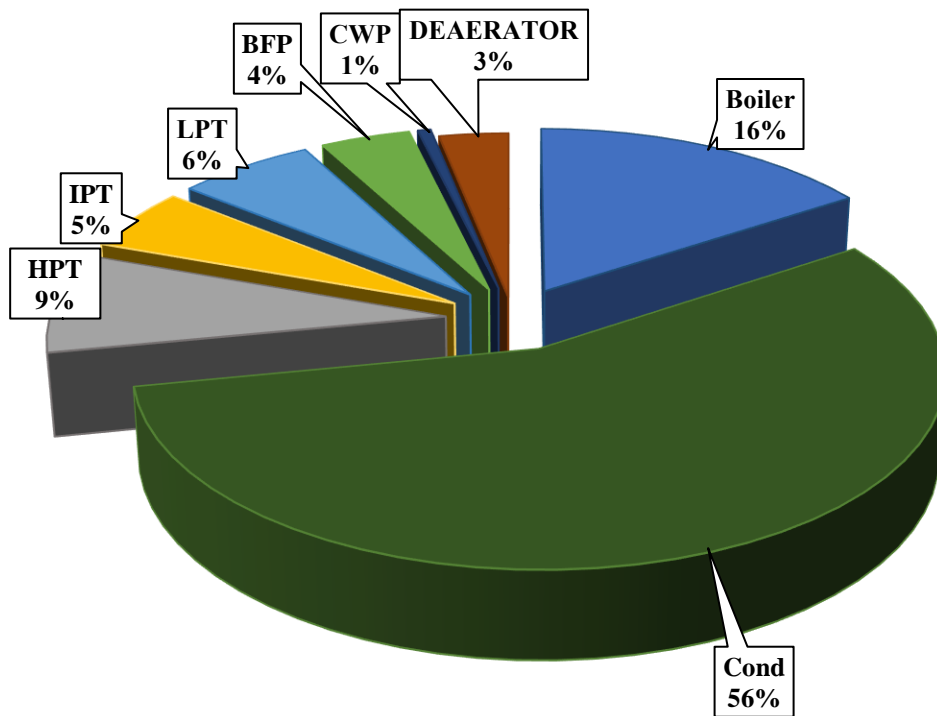


Figure 3. Energy losses percentages distribution at rated load

Figure 4 illustrates the exergy destruction across various components of the power plant, highlighting the areas where the most significant

losses occur. The boiler is the largest contributor, with an exergy destruction of 363.493 MW, accounting for 84.14% of the total

irreversibility of the thermal cycle. This high level of irreversibility is primarily due to heat transfer to the working fluid, losses from flue gas emissions, and chemical reactions in the furnace. These findings align with the research by Eke et al. [15], which reported that the boiler was responsible for 87% of total exergy destruction in a 220 MW thermal power plant. The boiler's high exergy destruction indicates that improving combustion efficiency and heat transfer in this component could yield substantial gains in overall system performance. In contrast, the condenser contributes 16.621 MW to exergy destruction, representing 3.85% of total irreversibility. This relatively low percentage is due to the lower quality of exergy destroyed in the condenser compared to other components.

The relatively low exergy destruction in the condenser highlights its lesser role in irreversibility, though attention to improving steam quality could still be beneficial.

The High-Pressure Turbine (HPT) experiences an exergy destruction of 14 MW, or 3.24% of the total exergy destruction, which is notably higher than the Intermediate-Pressure Turbine (IPT), with an exergy destruction of 9.474 MW (2.19%). This difference arises from the pressure drop and expansion processes, as the steam entering the HPT has a work potential of 271.088 MW, but only 20.33% of it is converted into useful work, resulting in greater exergy destruction compared to the IPT and the Low-Pressure Turbine (LPT). Interestingly, the

exergy destruction in the LPT is slightly higher than in the IPT, as irreversibility tends to increase at lower pressures where steam approaches the saturation line. Overall, the turbine subsystem contributes over 14% of the total exergy destruction, making it the second-largest source of irreversibility after the boiler. Turbines show significant potential for improvement, particularly by addressing pressure drop and maximizing the conversion of steam energy into useful work.

Auxiliary components, such as the boiler feed pump (BFP), cooling water pump (CWP), deaerator, and low-pressure heaters (LPH-1 to LPH-4), also contribute to exergy destruction. Combined, these components account for around 4.17% of the total exergy destruction, reflecting their supporting role in maintaining the thermal cycle. Among these, LPH-4 has an exergy destruction of 0.9262 MW (0.21%), which is higher due to the larger temperature difference between the extraction steam and the condensate water. Auxiliary components play a smaller but still meaningful role in the plant's overall exergy losses, suggesting incremental improvements across the board could further optimize the system.

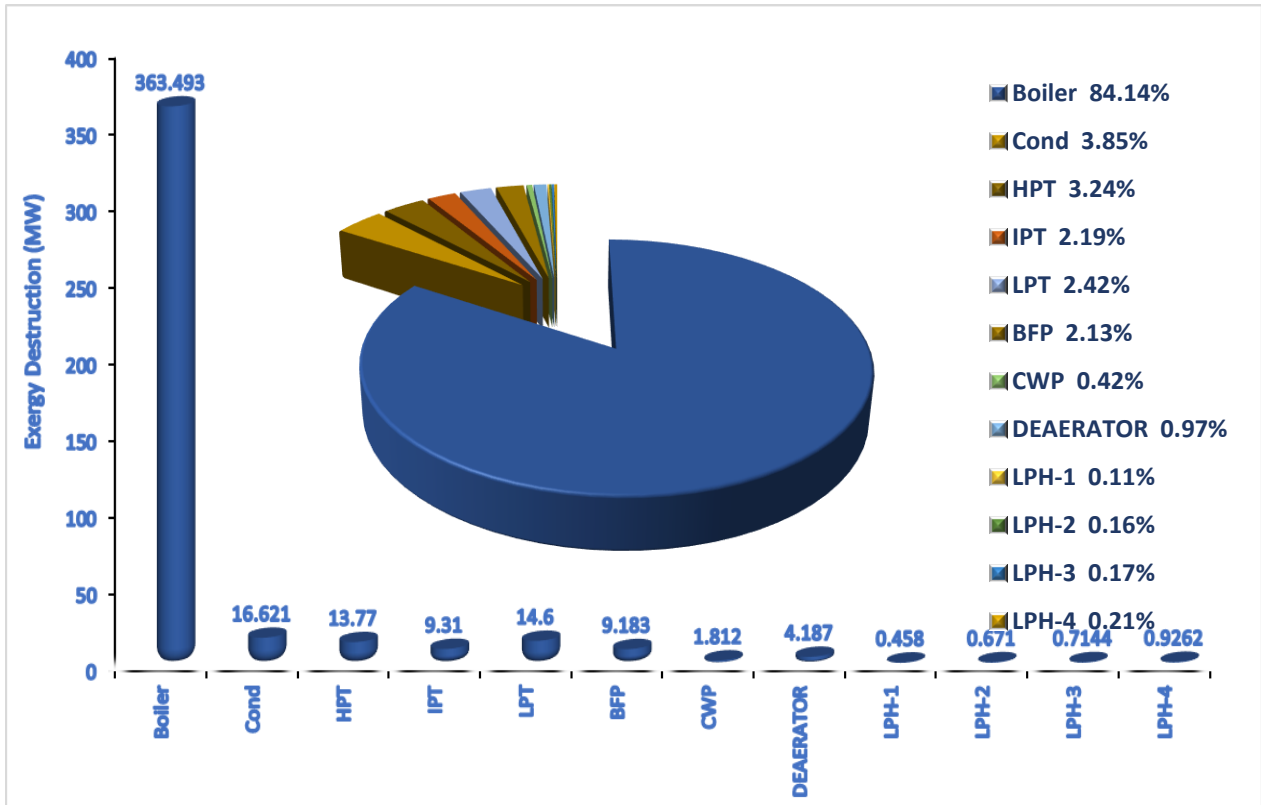


Figure 4. Exergy destruction distribution for real load.

Figure 5 shows the second law efficiency of various components. The Intermediate-Pressure Turbine (IPT) exhibits the best performance, utilizing only 9.58% of the steam's work potential, while the High-Pressure Turbine (HPT) wastes 20.6%, which is higher than the Low-Pressure Turbine's (LPT) waste of 10.87%. Understanding the second law efficiency of the turbines is crucial for optimizing energy use and improving overall system efficiency. Turbine performance is key to maximizing the overall energy efficiency of the system, and focusing on reducing energy waste in these components could provide substantial gains. Among the

feedwater heaters, LPH1 has the lowest efficiency at 66.28%, whereas LPH4 has the highest efficiency at 84.83%. The deaerator achieves 88.8% efficiency, while the boiler's efficiency is 44.52%. The condenser operates with a second law efficiency of 21.43%, and the feedwater pump is considerably more efficient at 40.14% compared to the condensate pump, which has an efficiency of 21.59%. The variation in feedwater heater efficiency also suggests that optimizing the lower-performing units, like LPH1, could help reduce irreversibility and enhance the plant's overall efficiency.

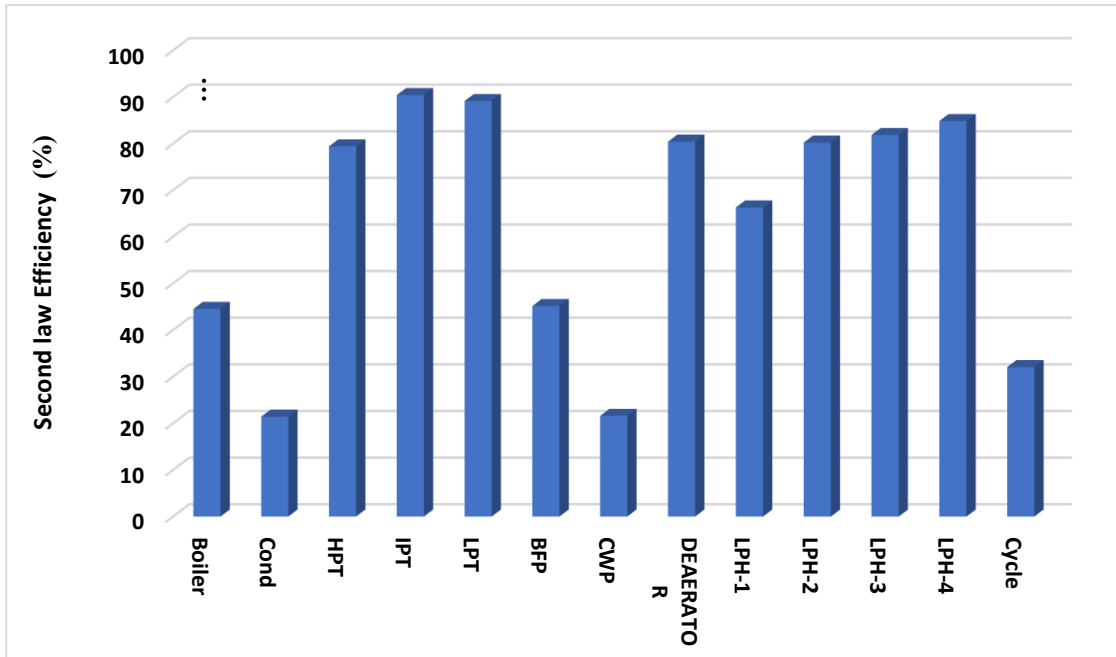


Figure 5. Second law Efficiency of the components

Figure 6 presents the energy efficiency of various components within the power plant. The Intermediate-Pressure Turbine (IPT) exhibits an energy efficiency of 83.71%, while the condenser has the lowest efficiency, slightly below 70%. The Low-Pressure Turbine (LPT) has an energy efficiency of 81.2%, which is approximately 10% lower than that of the boiler. The deaerator achieves the highest energy efficiency at 96.13%. Both the condensate extraction pump (CEP) and the boiler feed pump (BFP) show nearly identical efficiencies, differing by just 0.2%. The High-Pressure Turbine (HPT) has an energy efficiency of

around 67%, primarily due to insufficient utilization of thermal energy in the supplied steam, as suggested by the temperature of the steam exiting the turbine. Improving the HPT's thermal energy utilization could significantly increase its efficiency, while attention to the condenser's performance may yield further gains. The high efficiency of the deaerator and the similarity between the CEP and BFP efficiencies suggest that these systems are well-optimized, though minor improvements in the pumps could still contribute to overall performance.

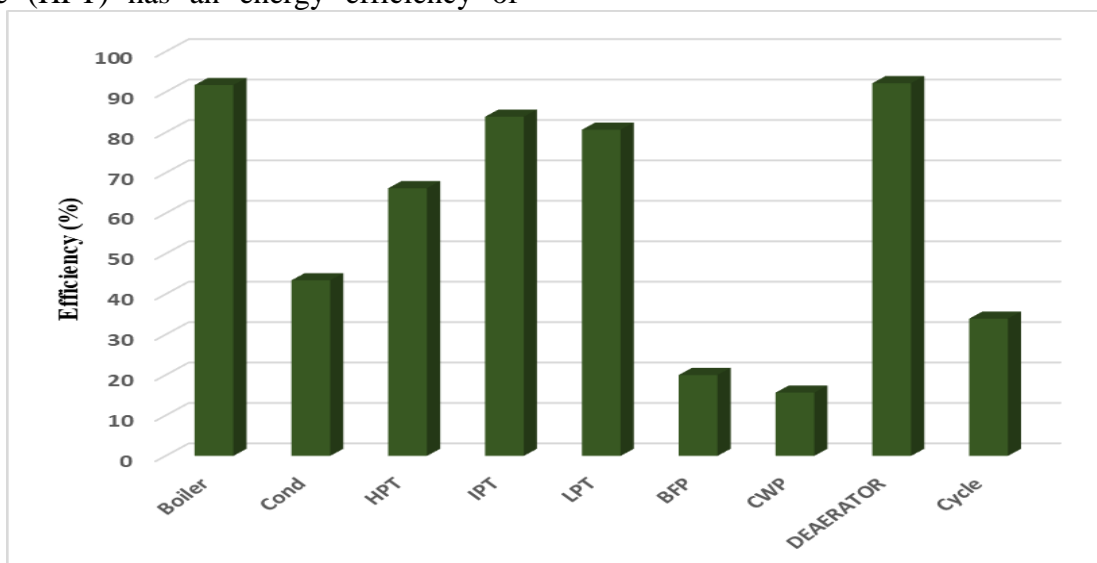


Figure 6. Energy Efficiency of the components

Figure 7 illustrates the exergy destruction of the condenser in a thermal power plant as ambient temperature increases from 20°C to 45°C. Exergy destruction in the condenser decreases from 15.74 MW at 20°C to 11.44 MW at 45°C, reflecting a decline with rising temperatures. This reduction is attributed to a smaller temperature difference between the condenser and the environment, leading to lower heat rejection and reduced exergy destruction. The condenser operates more efficiently at higher ambient temperatures due to the lower driving force for heat transfer, which minimizes irreversibilities caused by large temperature gradients. This behavior is consistent with previous research by Kopac and Hilalci [34], who observed a similar decrease in condenser exergy destruction as ambient temperature increased from 278 K to 308 K.

Conversely, exergy destruction increased for several components as ambient temperature rose from 20°C to 45°C. The Boiler Feed Pump (BFP) saw an 8.52% increase, the High-Pressure

Turbine (HPT) 8.54%, and the Intermediate-Pressure Turbine (IPT) 8.53%, reflecting higher irreversibilities due to less efficient expansion and increased pumping work. In contrast, the Deaerator (DTR) experienced an 11.94% reduction in exergy destruction, indicating improved efficiency in the deaeration process at higher temperatures. The results indicate that while rising ambient temperatures improve condenser and deaerator efficiency, they negatively affect turbines and pumps due to increased irreversibilities. This highlights the trade-offs in thermal plant performance under varying environmental conditions, pointing to potential areas for optimization in both turbines and auxiliary systems

These findings align with recent studies, such as Aljundi [19], which found that turbine exergy destruction increases with rising temperatures due to decreased isentropic efficiency, while auxiliary components like deaerators benefit from improved thermal performance in warmer conditions.

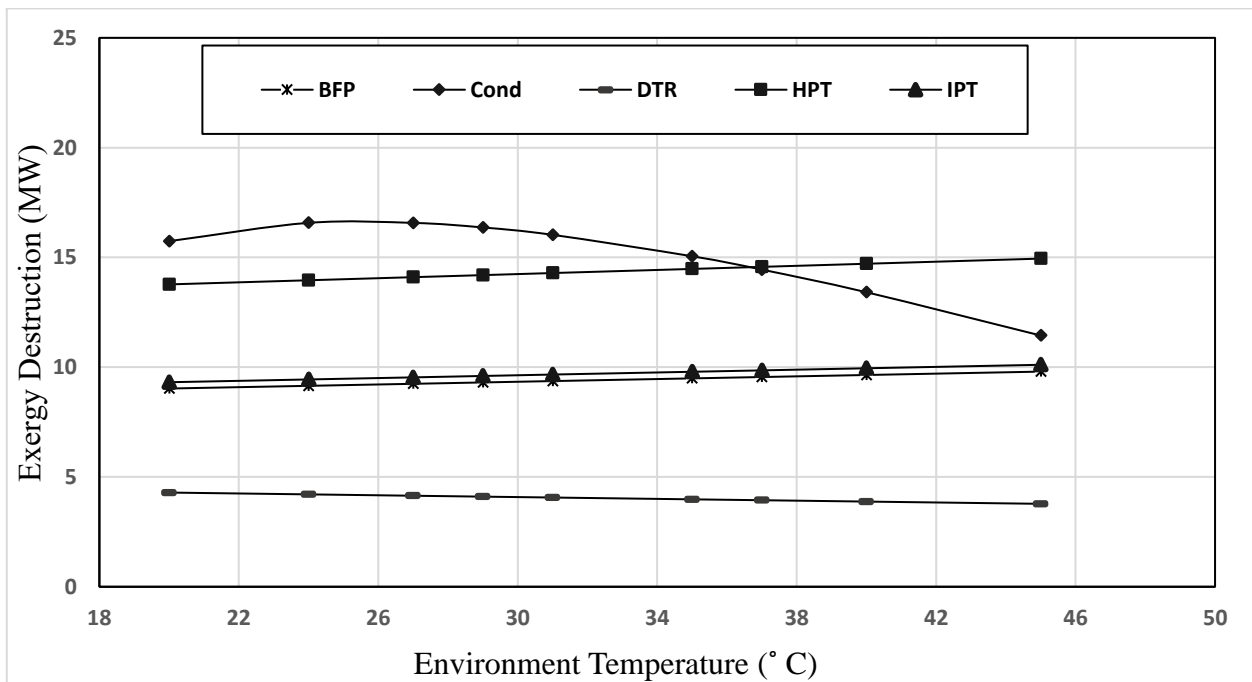


Figure 7. Effect of environment temperature on exergy destruction for main components at rated load

Figure 8 shows how ambient temperature variations between 20°C and 45°C impact exergy dissipation in thermal power plant heat exchangers. At lower temperatures (20°C), exergy destruction for LPH-1, LPH-2, LPH-3, and LPH-4 is 0.4503 MW, 0.6597 MW, 0.7024

MW, and 0.9106 MW, respectively. This is due to a favorable temperature gradient, which improves heat transfer efficiency. As temperatures increase to 45°C, exergy destruction decreases slightly, reflecting improved heat exchanger efficiency. However,

at very high temperatures, operational inefficiencies may occur, suggesting that extreme conditions could undermine performance. The variation in exergy destruction highlights the role of maintaining an optimal temperature gradient for efficient heat exchange. The results indicate that lower

temperatures promote better heat exchange efficiency due to larger temperature gradients. While increasing ambient temperatures initially improve efficiency, extreme heat may disrupt the performance of heat exchangers, signaling the importance of optimizing temperature management in power plants.

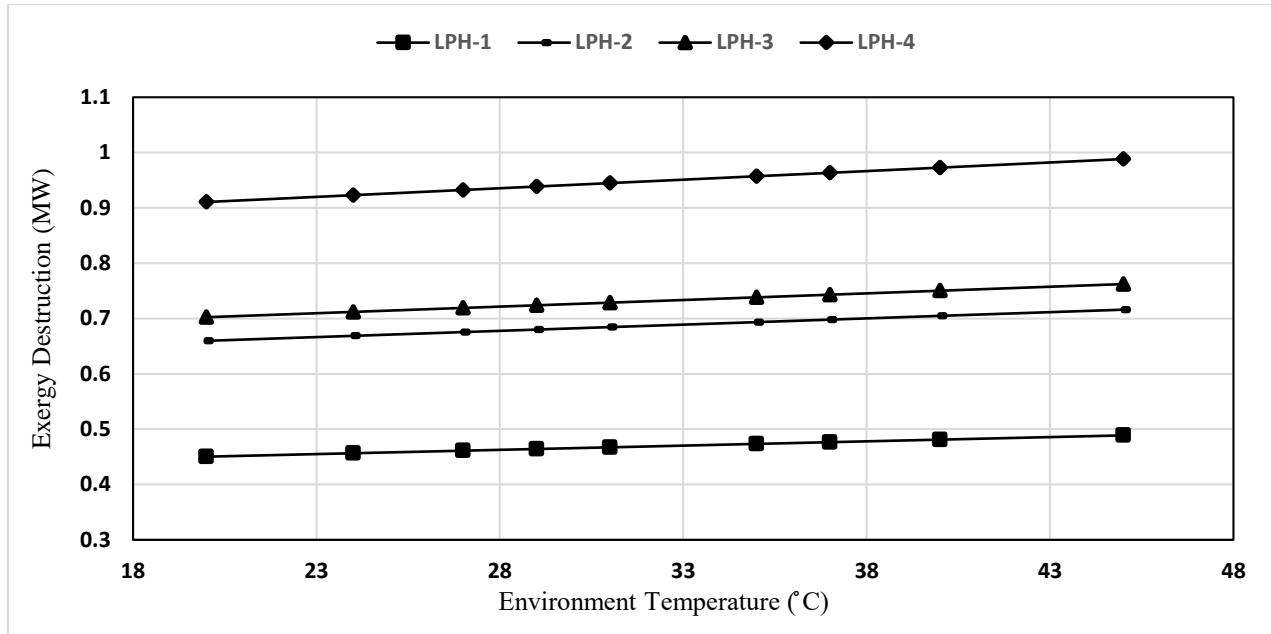


Figure 8. Effect of environment temperature on exergy destruction for (LPH-1-4) at rated load

Figure 9 illustrates how the efficiency of thermal power plant components declines as ambient temperatures increase, largely due to greater cooling demands and heat losses. Boiler efficiency drops by 7.4%, from 45.23% at 20°C to 41.87% at 45°C, as higher temperatures exacerbate heat loss and reduce combustion efficiency. Similarly, the High-Pressure Turbine (HPT) sees a 1.7% decline in efficiency (from 79.67% to 78.32%), and the Intermediate-Pressure Turbine (IPT) experiences a 0.8% decrease (from 90.56% to 89.84%), primarily

due to altered steam properties and heightened cooling requirements. Overall, the plant's efficiency falls by 1.2%, from 32.89% to 31.69%, underscoring the need for improved heat management to maintain performance under varying environmental conditions. The decrease in efficiency highlights the sensitivity of power plant performance to ambient temperature changes. Effective cooling and heat management strategies become critical as temperatures rise, in order to mitigate losses and maintain operational efficiency.

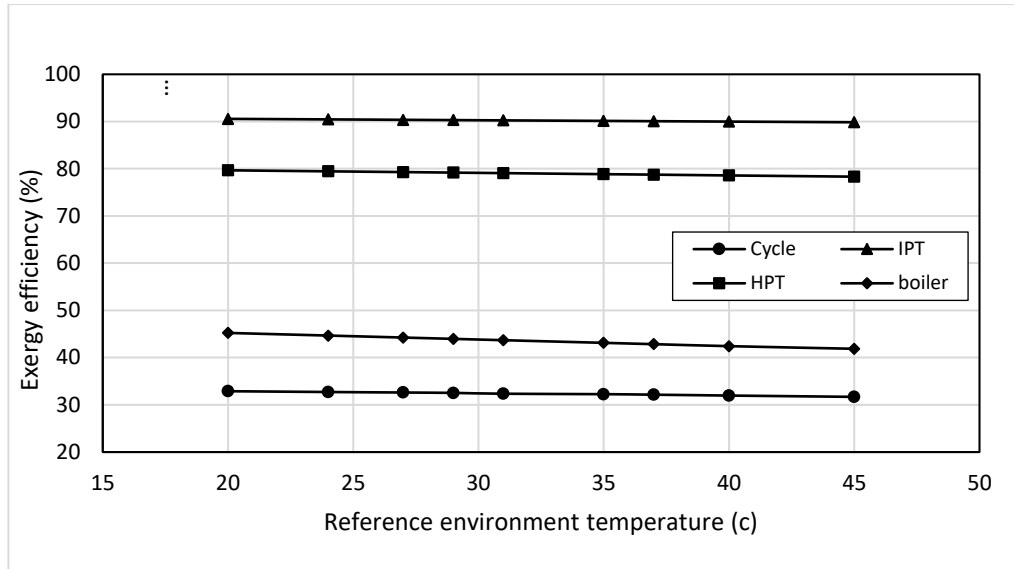


Figure 9. Effect of environment temperature on the efficiency of thermal power plant components

4.2. Analysis of Environmental emissions

The analytical results show that CO₂ emissions from burning crude oil, measured per kilogram of fuel, rise as ambient temperatures increase. As thermal power plants become less efficient at higher temperatures, emissions of both CO₂ and SO₂ increase. Figure 10 illustrates that CO₂ emissions rose from 51.8 kg/h at 20°C to 56.9 kg/h at 45°C, a 9.8% increase. Similarly, SO₂ emissions slightly increased from 1.02 kg/h to 1.03 kg/h over the same temperature range. The rise in CO₂ emissions contributes to global warming, intensifying climate change and

extreme weather events. The increase in SO₂ concentrations leads to air pollution, acid rain, and respiratory problems, harming both human health and ecosystems. Furthermore, higher fuel consumption drives up operating costs and may result in regulatory penalties, emphasizing the urgent need for efficiency improvements and cleaner energy alternatives. The rising emissions with increasing temperatures highlight the environmental and financial impacts of inefficiency in thermal power plants. This underscores the importance of adopting technologies to enhance efficiency and reduce reliance on fossil fuels to mitigate climate change and its associated costs.

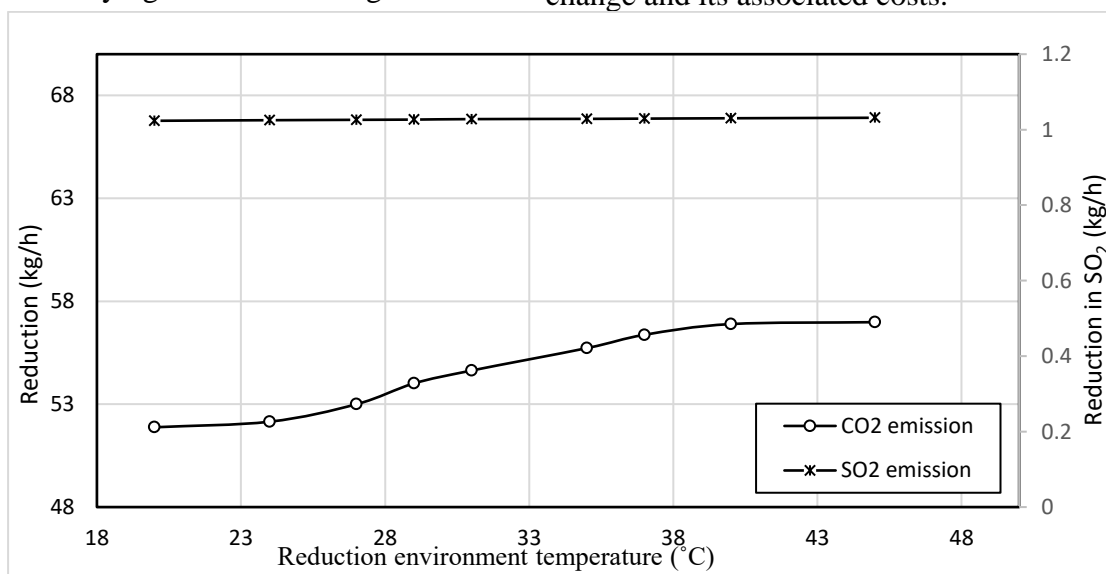


Figure 10. Impact of Environmental Temperature on Emissions

5. Conclusion

This study evaluates the energy, exergy, and environmental emissions of a 200 MW crude oil-fired power plant, emphasizing critical components such as the boiler, turbines, and heat exchangers. Utilizing ASPEN HYSYS software, the research quantifies energy and exergy losses, efficiency, and overall plant performance for the AL-Musayib SPP. Additionally, it assesses exergy destruction and efficiency in significant components like the combustion chamber, condenser, and turbines across a range of ambient temperatures (25°C to 45°C). The findings highlight key issues, including the identification of heat and energy losses and the influence of temperature on exergy destruction. The following conclusions can be drawn from the results.

- The condenser is the largest source of energy loss in the system, accounting for 181.76 MW (56.18%), primarily due to heat expulsion and low steam quality.
- The boiler contributes 51.08 MW (15.79%) to total losses from combustion

inefficiencies, while the high-pressure turbine (HPT), intermediate-pressure turbine (IPT), and low-pressure turbine (LPT) account for 27.50 MW (8.50%), 17.13 MW (5.29%), and 20.47 MW (6.33%), respectively.

- The boiler is the primary source of exergy destruction in the power plant, accounting for 84.14% of total irreversibility.
- The energy efficiency analysis reveals that while the Intermediate-Pressure Turbine (IPT) and deaerator perform well at 83.71% and 96.13% efficiency, respectively, the High-Pressure Turbine (HPT) lags at around 67%.
- The overall cycle efficiency is 33.9%, with exergy efficiency of 32.89%.
- the analysis revealed that as the ambient temperature increased from 20°C to 45°C, CO₂ emissions rose from 51.8 kg/h to 56.9 kg/h, and SO₂ emissions also experienced a slight increase from 1.02 kg/h to 1.03 kg/h.

NOMENCLATURE		
Terms	Description	Units
e	Specific energy	(kJ/kg)
E	Total Energy	(kJ)
EX	Flow Exergy	(kW)
EXP	Expansion Valve	-
G	The gravity of the earth	(m/s ²)
GV	Governing Valve	-
\dot{m}	Mass Flow Rate	(kg/s)
P	Pressure	(bar)
Q	Heat	(kW)
QI	Heat loss	(kW)
T	Temperature	(°C)
s	Specific entropy	(kJ/kg-K)
W	Work	(kW)
η_I	First law efficiency	
η_{II}	Second law efficiency	
ψ	Specific Exergy	(kJ/kg)
h	Specific Enthalpy	(kJ/kg)
HPH	High Pressure Heater	-
HPT	High Pressure Turbine	-
IPT	Intermediate Pressure Turbine	-
I destroyed	Destroyed Exergy	(kW)
LPH	Low Pressure Heater	kPa
LPT	Low Pressure Turbine	-
\dot{m}_f	mass of fuel and air	(kg/s)
CFWH	closed feed water heater	-
Subscripts		
0	Reference state	
a	Air	
des	Destroyed	
g	Gas	
i	Inlet	
o	Outlet	

References

- [1] M.R. Hasan, entropy method as criteria for analysis a steam power plant, *Journal of Engineering* 15 (2009) 4025–4040. <https://doi.org/10.31026/j.eng.2009.03.15>.
- [2] H.H. Erdem, A.V. Akkaya, B. Cetin, A. Dagdas, S.H. Sevilgen, B. Sahin, I. Teke, C. Gungor, S. Atas, Comparative energetic and exergetic performance analyses for coal-fired thermal power plants in Turkey, *International Journal of Thermal Sciences* 48 (2009) 2179–2186. <https://doi.org/10.1016/j.ijthermalsci.2009.03.007>.
- [3] S.M. Shakir, A.A. Farhan, Movable Thermal Screen For Saving Energy Inside The Greenhouse, *Association of Arab Universities Journal of Engineering Sciences* 26 (2019) 106–112. <https://doi.org/10.33261/jaaru.2019.26.1.014>.
- [4] O.J. Khaleel, F. Basim Ismail, T. Khalil Ibrahim, S.H. bin Abu Hassan, Energy and exergy analysis of the steam power plants: A comprehensive review on the Classification, Development, Improvements, and configurations, *Ain Shams Engineering Journal* 13 (2022) 101640. <https://doi.org/10.1016/j.asej.2021.11.009>.
- [5] E. Ersayin, L. Ozgener, Performance analysis of combined cycle power plants: A case study, *Renewable and Sustainable Energy Reviews* 43 (2015) 832–842. <https://doi.org/10.1016/j.rser.2014.11.082>.
- [6] M.A. Rosen, D.S. Scott, Entropy production and exergy destruction: Part I—hierarchy of Earth's major constituencies, *Int J Hydrogen Energy* 28 (2003) 1307–1313. [https://doi.org/10.1016/S0360-3199\(03\)00026-0](https://doi.org/10.1016/S0360-3199(03)00026-0).
- [7] M.A. Rosen, Exergy Analysis as a Tool for Addressing Climate Change, *European Journal of Sustainable Development Research* 5 (2021) em0148. <https://doi.org/10.21601/ejosdr/9346>.
- [8] J.A.M. da Silva, S. Ávila Filho, M. Carvalho, Assessment of energy and exergy efficiencies in steam generators, *Journal of the Brazilian Society of Mechanical Sciences and Engineering* 39 (2017) 3217–3226. <https://doi.org/10.1007/s40430-016-0704-6>.
- [9] E. Arabaci, B. Kiliç, Specific network and mean effective pressure based thermodynamic analysis and optimization of ideal atkinson cycle, *Konya Journal of Engineering Sciences* 10 (2022) 1035–1047. <https://doi.org/10.36306/konjes.1120243>.
- [10] M.K. Mohammed, W.H. Al Doori, A.H. Jassim, T.K. Ibrahim, A.T. Al-Sammarraie, Energy and exergy analysis of the steam power plant based on effect the numbers of feed water heater, *Journal of Advanced Research in Fluid Mechanics and Thermal Sciences* 56 (2019) 211–222.
- [11] O.J. Khaleel, T.K. Ibrahim, F.B. Ismail, S.H.A. Hassan, Thermal Performance of Coal-Fired Power Plant based on Number of Feedwater Heaters, *Journal of Advanced Research in Fluid Mechanics and Thermal Sciences* 95 (2022) 188–205. <https://doi.org/10.37934/arfmts.95.1.188205>.
- [12] O.J. Khaleel, T.K. Ibrahim, F.B. Ismail, A.T. Al-Sammarraie, Developing an analytical model to predict the energy and exergy based performances of a coal-fired thermal power plant, *Case Studies in Thermal Engineering* 28 (2021) 101519. <https://doi.org/10.1016/j.csite.2021.101519>.
- [13] T.K. Ibrahim, M.K. Mohammed, O.I. Awad, A.N. Abdalla, F. Basrawi, M.N. Mohammed, G. Najafi, R. Mamat, A comprehensive review on the exergy analysis of combined cycle power plants, *Renewable and Sustainable Energy Reviews* 90 (2018) 835–850. <https://doi.org/10.1016/j.rser.2018.03.072>.
- [14] V. Kumar, V.K. Saxena, R. Kumar, S. Kumar, Energy, exergy, sustainability and environmental emission analysis of coal-fired thermal power plant, *Ain Shams Engineering Journal* 15 (2024) 102416. <https://doi.org/10.1016/j.asej.2023.102416>.
- [15] M.N. Eke, D.C. Onyejekwe, O.C. Iloeje, C.I. Ezekwe, P.U. Akpan, Energy and exergy evaluation of a 220MW thermal power plant, *Nigerian Journal of Technology* 37 (2018) 115. <https://doi.org/10.4314/njt.v37i1.15>.
- [16] S.C. Kaushik, V.S. Reddy, S.K. Tyagi, Energy and exergy analyses of thermal power plants: A review, *Renewable and Sustainable Energy Reviews* 15 (2011) 1857–1872. <https://doi.org/10.1016/j.rser.2010.12.007>.
- [17] M. Ameri, P. Ahmadi, A. Hamidi, Energy, exergy and exergoeconomic analysis of a steam power plant: A case study, *Int J Energy Res* 33 (2009) 499–512. <https://doi.org/10.1002/er.1495>.
- [18] H. Ghaebi, M. Amidpour, S. Karimkashi, O. Rezayan, Energy, exergy and thermoeconomic analysis of a combined cooling, heating and power (CCHP) system with gas turbine prime mover, *Int J Energy Res* 35 (2011) 697–709. <https://doi.org/10.1002/er.1721>.
- [19] I.H. Aljundi, Energy and exergy analysis of a steam power plant in Jordan, *Appl Therm Eng* 29 (2009) 324–328. <https://doi.org/10.1016/j.applthermaleng.2008.02.029>.
- [20] G.R. Ahmadi, D. Toghraie, Energy and exergy analysis of Montazeri Steam Power Plant in Iran, *Renewable and Sustainable Energy Reviews* 56 (2016) 454–463. <https://doi.org/10.1016/j.rser.2015.11.074>.
- [21] T. Nakaishi, Developing effective CO₂ and SO₂ mitigation strategy based on marginal abatement costs of coal-fired power plants in China, *Appl Energy* 294 (2021) 116978. <https://doi.org/10.1016/j.apenergy.2021.116978>.
- [22] E. Ahmadian, R.R. Schmidt, Exergy analysis of district energy systems and comparison of their exergetic, energetic and environmental performance, *International Journal of Exergy* 32 (2020) 103. <https://doi.org/10.1504/IJEX.2020.108169>.

- [23] M. Akbari Wakilabadi, M. Bidi, A.F. Najafi, Energy, Exergy analysis and optimization of solar thermal power plant with adding heat and water recovery system, *Energy Convers Manag* 171 (2018) 1639–1650. <https://doi.org/10.1016/j.enconman.2018.06.094>.
- [24] A.A.A. Abuelnuor, M.M. Hassan Suliman, M.A. Abuelnuor, O. Younis, E.F. Mohamed, Exergy analysis of the boiler in phase 3 of the Khartoum North power plant, *Results in Engineering* 21 (2024) 101919. <https://doi.org/10.1016/j.rineng.2024.101919>.
- [25] K. Ansari, H. Sayyaadi, M. Amidpour, Thermoeconomic optimization of a hybrid pressurized water reactor (PWR) power plant coupled to a multi effect distillation desalination system with thermo-vapor compressor (MED-TVC), *Energy* 35 (2010) 1981–1996. <https://doi.org/10.1016/j.energy.2010.01.013>.
- [26] O. Shamet, R. Ahmed, K. Nasreldin Abdalla, Energy and Exergy Analysis of a Steam Power Plant in Sudan, *African Journal of Engineering & Technology* 1 (2021). <https://doi.org/10.47959/AJET.2021.1.1.4>.
- [27] W.A. Salih, A.A. Alkumait, H.J. Khalaf, Energy And Exergy Assessment of North Refineries Company (NRC) Steam Cycle Based on Air Mass Flowrate of Main Condenser, *Tikrit Journal of Engineering Sciences* 28 (2021) 61–70. <https://doi.org/10.25130/tjes.28.3.05>.
- [28] M. Tavana, M. Deymi-Dashtebayaz, D. Dadpour, B. Mohseni-Gharyehsafa, Realistic Energy, Exergy, and Exergoeconomic (3E) Characterization of a Steam Power Plant: Multi-Criteria Optimization Case Study of Mashhad Tous Power Plant, *Water (Basel)* 15 (2023) 3039. <https://doi.org/10.3390/w15173039>.
- [29] M. Akhoundi, M. Deymi-Dashtebayaz, E. Tayyeban, H. Khabbazi, Parametric study and optimization of the precooled Linde–Hampson (PCLH) cycle for six different gases based on energy and exergy analysis, *Chemical Papers* 77 (2023) 5343–5356. <https://doi.org/10.1007/s11696-023-02866-5>.
- [30] Y. Zhang, T. Liu, M. Guang, W. Fu, B. Li, Exergy, can it be used to reflect the environmental issues of a fuel, *International Journal of Exergy* 40 (2023) 1. <https://doi.org/10.1504/IJEX.2023.128516>.
- [31] T.J. Kotas, Exergy concepts for thermal plant, *Int J Heat Fluid Flow* 2 (1980) 105–114. [https://doi.org/10.1016/0142-727X\(80\)90028-4](https://doi.org/10.1016/0142-727X(80)90028-4).
- [32] A. Naseeb, A. Ramadan, S.M. Al-Salem, Economic Feasibility Study of a Carbon Capture and Storage (CCS) Integration Project in an Oil-Driven Economy: The Case of the State of Kuwait, *Int J Environ Res Public Health* 19 (2022) 6490. <https://doi.org/10.3390/ijerph19116490>.
- [33] R.V. Padilla, R.G. Benito, W. Stein, An Exergy Analysis of Recompression Supercritical CO₂ Cycles with and without Reheating, *Energy Procedia* 69 (2015) 1181–1191. <https://doi.org/10.1016/j.egypro.2015.03.201>.
- [34] M. Kopac, A. Hilalci, Effect of ambient temperature on the efficiency of the regenerative and reheat Çatalağzı power plant in Turkey, *Appl Therm Eng* 27 (2007) 1377–1385. <https://doi.org/10.1016/j.applthermaleng.2006.10.029>.